

# Effect of Mechanical Grinding and Sonication on the Optical Properties of MoS<sub>2</sub> Nanosheets

Shweta<sup>a\*</sup>, Vinamrita Singh<sup>b</sup>, Kaushal Kumar<sup>a</sup>, Tanuj Kumar<sup>c</sup>, & Arun Kumar<sup>a</sup>

<sup>a</sup>Department of Physics, J C Bose University of Science & Technology YMCA, Faridabad 121 006, India

<sup>b</sup>Department of Physics, Netaji Subhas University of Technology, East Campus, Delhi 110 031, India

<sup>c</sup>Department of Nanosciences & Materials, Central University of Jammu, Jammu and Kashmir 181 143, India

Received: 9 August 2023; Accepted: 26 September 2023

In the present study, MoS<sub>2</sub> nanosheets are prepared by a two-step, grinding-assisted ultrasonication technique. Various parameters governing the optical, electrical, and dielectric properties of the MoS<sub>2</sub> nanosheets are determined from the absorbance, reflectance, and transmittance spectra acquired using UV-Vis spectroscopy. These parameters are analysed with change in grinding hours as well as for sonication effects. It is observed that the absorption coefficient, optical conductivity, and dissipation factor increase (along with a decrease in refractive index) with increase in grinding hours and with sonication. The obtained changes in the optical parameters are correlated with the number of exfoliated layers revealed by Raman spectroscopy. The results of this study provide insightful information about the layer-dependent properties of MoS<sub>2</sub> nanosheets and develop better understanding of how the synthesis routes are effective for tailoring the optical response of MoS<sub>2</sub> nanosheets.

**Keywords:** Exfoliation, Molybdenum Disulphide (MoS<sub>2</sub>), Optical Properties, UV-Vis Spectroscopy

## 1 Introduction

Over recent years, two-dimensional materials have attracted researchers because of their captivating, versatile properties, and potential for industrial applications. Among various 2D materials, molybdenum disulphide (MoS<sub>2</sub>) is emerging as a super material for its tunable electronic and optical properties. MoS<sub>2</sub> has layer-dependent, tailorable energy bandgap ( $E_g$ ) values in UV-NIR range (bulk and indirect  $E_g \sim 1.3$  eV, monolayer and direct  $E_g \sim 1.9$ -2.3 eV) and being suitable for optoelectronic applications.<sup>1-3</sup>

For synthesis of MoS<sub>2</sub> nanosheets, various physical and chemical approaches have been briefed by Sun *et al.*<sup>4</sup> Among the many available methods, liquid exfoliation via ultrasonication is adopted owing to its ease, cost-effectiveness, no structural changes, and tailorable thickness of exfoliated layers as mentioned in our previous work.<sup>1</sup> For application point of view, the study of optical and electrical properties of 2D MoS<sub>2</sub> is crucial. In literature, the optical properties of 2D MoS<sub>2</sub> have been studied and analysed by many researchers employing different techniques, such as ellipsometry, UV spectroscopy, computational

models, etc.<sup>2,3,5-8</sup> Yet, little is known about all the optical parameters – absorption coefficient ( $\alpha$ ), extinction coefficient (K), energy bandgaps ( $E_g$ ), refractive index ( $\eta$ ), optical conductivity, real part and imaginary part of the dielectric constant, and dissipation factor in a single frame especially for liquid exfoliated nanosheets. Moreover, the effects of mechanical grinding and sonication on optical properties have not been reported yet.

In this study, the MoS<sub>2</sub> nanosheets are prepared by two-step grinding-assisted liquid phase exfoliation process in N-Methylpyrrolidone (NMP) solvent. The grinding hours and sonication parameters are varied for assessing their effects on the optical properties of the prepared nanosheets. The real part and the imaginary part of the dielectric constants along with dissipation factor are calculated using  $\eta$  and K. The effects of grinding and sonication on the optical parameters may assist in the optimization of the processing parameters as per the required areas of application.

## 2 Materials and Methods

The MoS<sub>2</sub> nanosheets are prepared using the method highlighted previously.<sup>1</sup> In brief, 4 g of bulk MoS<sub>2</sub> powder (purity 99%, Nanoshel) is manually

\*Corresponding author (E-mail: shweta.aggarwal29@gmail.com)

grounded for 2 and 4 h in 1 ml of NMP solvent (99% purity, analytical grade, CDH). The grounded powders are dried at 60°C for 24 h. Four set of solutions are then prepared by mixing 1 g of MoS<sub>2</sub> with 20 ml of NMP solvent followed by stirring at 1000 rpm for 2 h. Two of these solutions are probe sonicated (LABSONIC Probe Sonicator, 1200W) for 2 h at 5°C (in an ice bath) with a 5s on and 2s off state to avoid heating. All four samples are left undisturbed for natural sedimentation followed by centrifuge at 5000 rpm for 30 minutes. Top 2/3<sup>rd</sup> portion of the supernatants are collected consisting of exfoliated MoS<sub>2</sub> nanosheets.

Structural analysis is carried out using Perkin-Elmer Spectrum Two FT-IR spectrometer. The absorbance, transmittance and reflectance of the samples are acquired using Shimadzu UV-3600i plus UV-VIS-NIR Spectrophotometer. For UV characterizations, the samples are coated on pre-cleaned glass substrates by drop-casting, followed by drying for 12 h at 60°C to remove the solvent.

### 3 Results and Discussion

#### 3.1 Structural analysis

The structural features in terms of the functional groups present in the prepared MoS<sub>2</sub> nanosheets is

studied using FTIR spectra shown in Fig. 1(a). It represents the comparative spectra of bulk and exfoliated nanosheets showing the Mo-S vibration peaks at 470 cm<sup>-1</sup> and ~460 cm<sup>-1</sup> for bulk and 2D MoS<sub>2</sub>, respectively. The Mo-S vibration peaks are weak in 2D MoS<sub>2</sub> due to the low yield of the suspensions. Two more broad peaks are detected corresponding to O-H bending vibrations (1660 cm<sup>-1</sup> to 1754 cm<sup>-1</sup> in 2D MoS<sub>2</sub>, 1648 cm<sup>-1</sup> for bulk MoS<sub>2</sub>) and H-O-H stretching vibrations (2955 cm<sup>-1</sup> and 2930 cm<sup>-1</sup> for exfoliated MoS<sub>2</sub> and bulk MoS<sub>2</sub>, respectively). The observed blue shift in the 2D MoS<sub>2</sub> peaks is due to the high energy sonication process causing residual stress in the dismantled layers.<sup>9,10</sup> The FTIR spectrum confirms the presence of MoS<sub>2</sub> with no structural alternations in the exfoliated nanosheets. In addition to this, the structural analysis by Raman spectroscopy, as shown in our previous work<sup>1</sup>, confirms the formation of nanosheets in mono and bi-layer range.

#### 3.2 Optical absorption studies

The optical properties of MoS<sub>2</sub> suspensions are investigated from the absorbance (A), reflectance (R), and transmittance (T) spectra obtained in the wavelength range of 300-800 nm as shown in Fig. 1(b-d). Figure 1(b) represents the comparison of

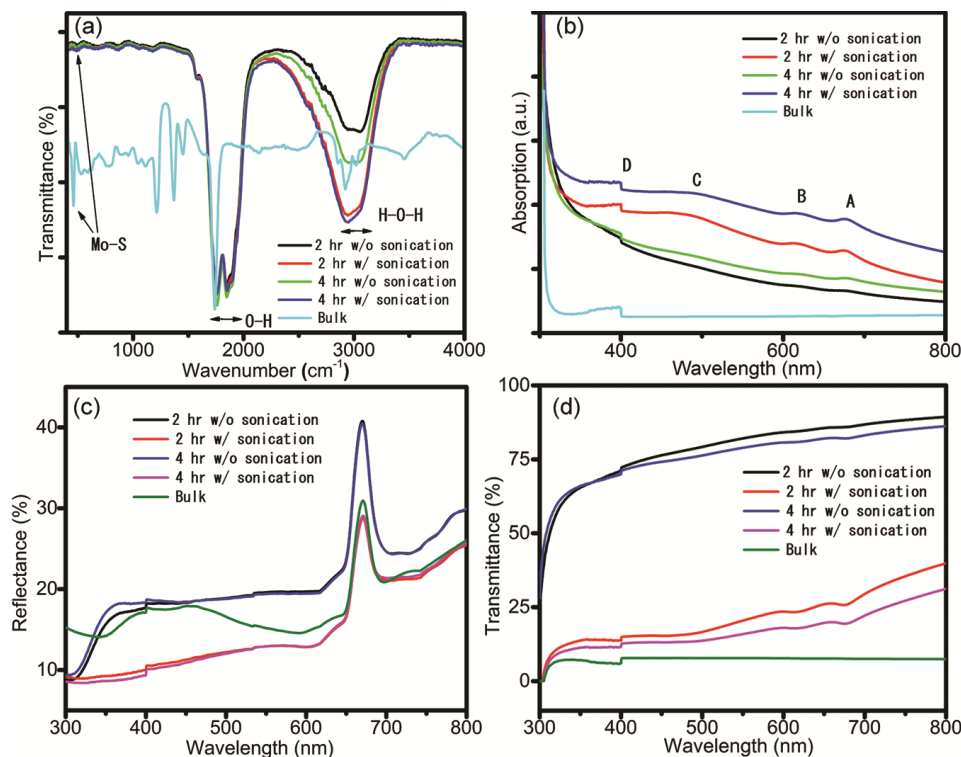


Fig. 1 — (a) FTIR spectra, (b) UV-Vis absorption, (c) reflectance, & (d) transmittance of bulk and exfoliated MoS<sub>2</sub> nanosheets.

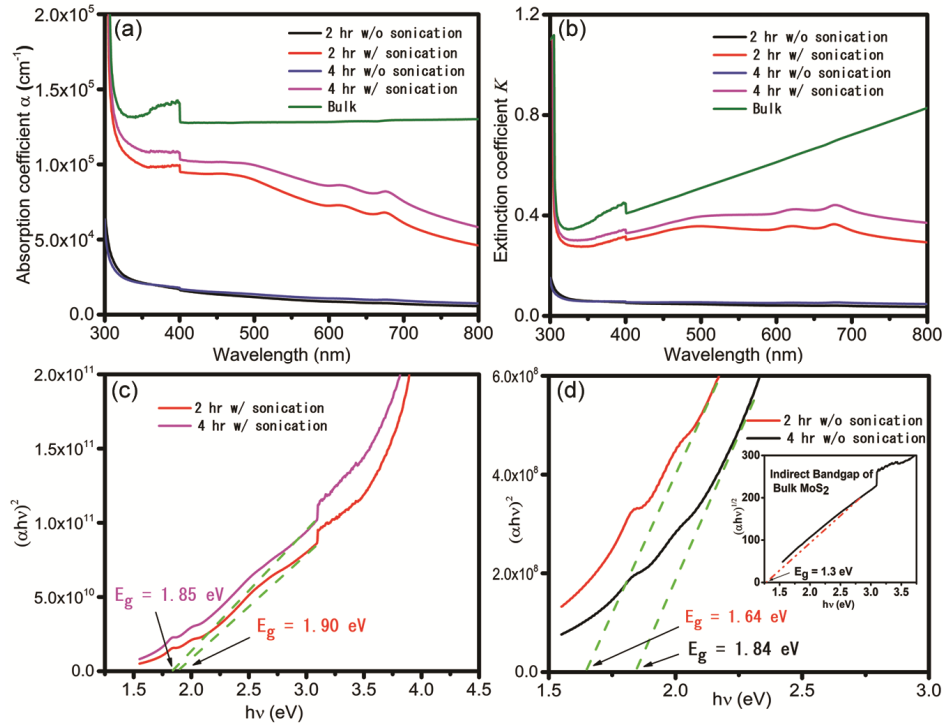


Fig. 2 — (a) Absorption coefficient, (b) extinction coefficient spectra of bulk and exfoliated MoS<sub>2</sub> nanosheets, (c) Tauc plots for direct bandgap of sonicated, & (d) direct bandgap of non-sonicated (bulk MoS<sub>2</sub> in inset) MoS<sub>2</sub> nanosheets.

exfoliated MoS<sub>2</sub> with its bulk counterpart in terms of characteristic excitonic peaks of MoS<sub>2</sub> - peaks A (~670 nm) and B (~613 nm) corresponding to the smallest direct electronic transition from the valence band (VB) top to the conduction band (CB) bottom. The peaks C (~480 nm) and D (~400 nm) depict the direct transition from deep VB to CB.<sup>11</sup> Few points that can be inferred from the absorption graph are: i) absorption is maximum for bulk MoS<sub>2</sub> but corresponds to indirect transitions only, ii) absorption is minimum with very feeble excitonic peaks for samples prepared without sonication, iii) sonicated samples show strong excitonic peaks depicting direct transitions along with good absorption values, and iv) besides the appearance of excitonic peaks, blue shifts of 1.5 nm in peak A and 1.0 nm in peak B are also observed for varying grinding hours from 2 hours to 4 hours for sonicated samples. This blue shift signifies an increase in the energy bandgap and thus effective reduction of MoS<sub>2</sub> into few layers.<sup>12</sup>

The reflectance spectra (Fig.1(c)) depict the small values of reflectance which is further reduced by employing sonication for exfoliation process with no visible effects of grinding hours. Fig. 1(d) shows the transmittance spectra of the synthesized nanosheets

and is complementary to the absorption spectra with minimum transmittance values of bulk MoS<sub>2</sub> and maximum for non-sonicated samples. From A, R and T curves, the MoS<sub>2</sub> nanosheets synthesized by 4 hours grinding-assisted sonication technique have enhanced absorption in the visible region.

### 3.3 Absorption coefficient and Extinction coefficient

Absorption coefficient ( $\alpha$ ) and extinction coefficient ( $K$ ) depend very strongly on the incident photon energy ( $h\nu$ ) and the  $E_g$ , and are calculated from UV spectroscopy measurements using Eq. (1) called Beer Lambert Law and Eq. (2), respectively.<sup>7</sup>

$$\alpha = \frac{\ln\left(\frac{I_0}{I}\right)}{t} = -\frac{\ln(T)}{t} = 2.303 \left(\frac{A}{t}\right) \quad \dots (1)$$

$$K = \frac{\alpha\lambda}{4\pi} \quad \dots (2)$$

where,  $I_0$  is the incident light intensity,  $I$  is the transmitted light intensity,  $\lambda$  is wavelength of light, and  $t$  is film thickness in cm.

The calculated absorption coefficient values are shown in Fig. 2(a), and the bulk MoS<sub>2</sub> has maximum absorption coefficient value, while it is minimum for

non-sonicated samples. In addition,  $\alpha$  value shows an increase with increasing grinding hours from 2 hours to 4 h. Since  $\alpha$  represents the absorption ability of a material, the 4 hours grinding and sonication is the most effective process to obtain 2D MoS<sub>2</sub> nanosheets.

The same behaviour for extinction coefficient (Fig. 2b), which deals with the fraction of light lost on scattering, is observed for the samples since it is directly proportional to  $\alpha$ .

**3.4 Optical energy bandgap**

Optical bandgap of the prepared nanosheets is computed from the Tauc’s relation. Figure 2(c) shows that the direct bandgap values for sonicated samples are ~1.9 eV while for non-sonicated samples the direct bandgap values are 1.64 eV and 1.84 eV for 2 hours and 4 hours grinding, respectively, as shown in Fig. 2(d) indicating formation of MoS<sub>2</sub> nanosheets.<sup>5</sup> The indirect bandgap for bulk MoS<sub>2</sub> (1.3 eV) is shown as an inset of Fig. 2(d). It is stated in the literature that with decrease in number of layers, the bandgap increases due to quantum confinement and intra-layer interaction.<sup>8</sup> Longer grinding hours lead to a decrease in the number of layers and hence an increase in the bandgap, while the bandgap of sonicated samples are not affected by the grinding hours.

**3.5 Refractive index**

The refractive index ( $\eta$ ) is estimated from the reflectance data obtained from UV-Vis spectroscopy using Eq. (3).<sup>13</sup> It is an important

factor providing information of light-matter interaction in 2D MoS<sub>2</sub>.

$$\eta = \frac{(1 + R^{\frac{1}{2}})}{(1 - R^{\frac{1}{2}})} \dots (3)$$

It can be seen from Fig. 3(a) that refractive index is minimum for sonicated samples with values equal to 3.34 (2 hours grinding) and 3.31 (4 hours grinding) at 670 nm corresponding to A exciton peak. This pattern of decrease in  $\eta$  with decreasing film thickness is similar to the other research reports.<sup>6</sup> The  $\eta$  of non-sonicated samples is higher than the bulk MoS<sub>2</sub> and can be attributed to the low degrees of disorders because of multi-layered structures.

**3.6 Optical conductivity**

To analyse the optical response of prepared nanosheets, another parameter is optical conductivity calculated using Eq. (4) and shown in Fig. 3(b).<sup>14</sup> The optical conductivity is following the same trend as absorption coefficient and refractive index vs. wavelength.

The maximum value of  $\sigma_{opt}$  obtained for exfoliated nanosheets is  $6.5 \times 10^{10} \text{ s}^{-1}$  at 670 nm for 4 hours grinding and with sonication. Such a high value of optical conductivity denotes high photo-response of the sample because of its high absorbance.

$$\sigma_{opt} = \frac{\alpha \eta c}{4\pi} \dots (4)$$

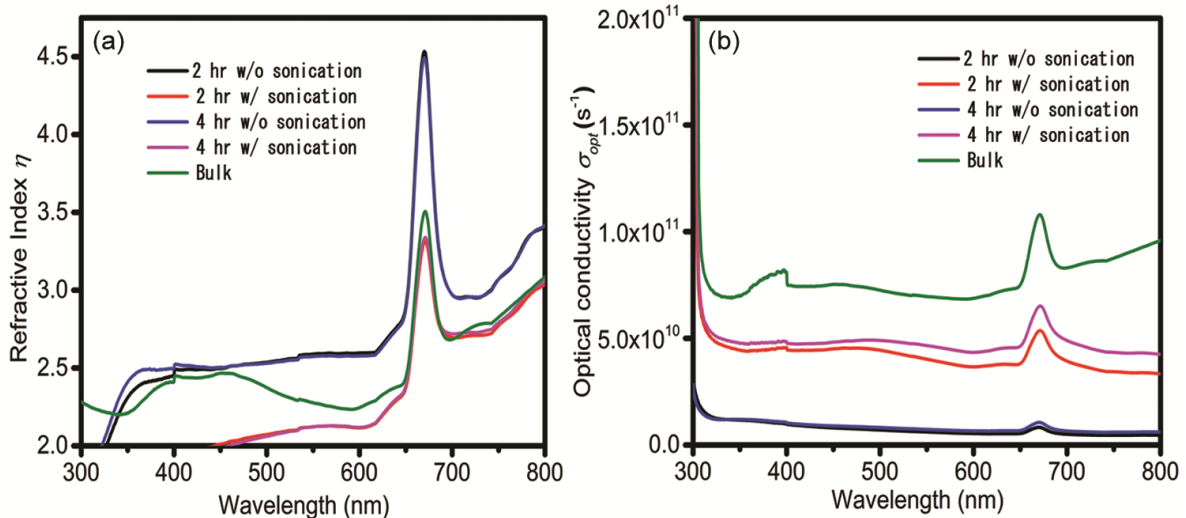


Fig. 3 — (a) Refractive index and (b) optical conductivity of bulk MoS<sub>2</sub> and exfoliated MoS<sub>2</sub> nanosheets.

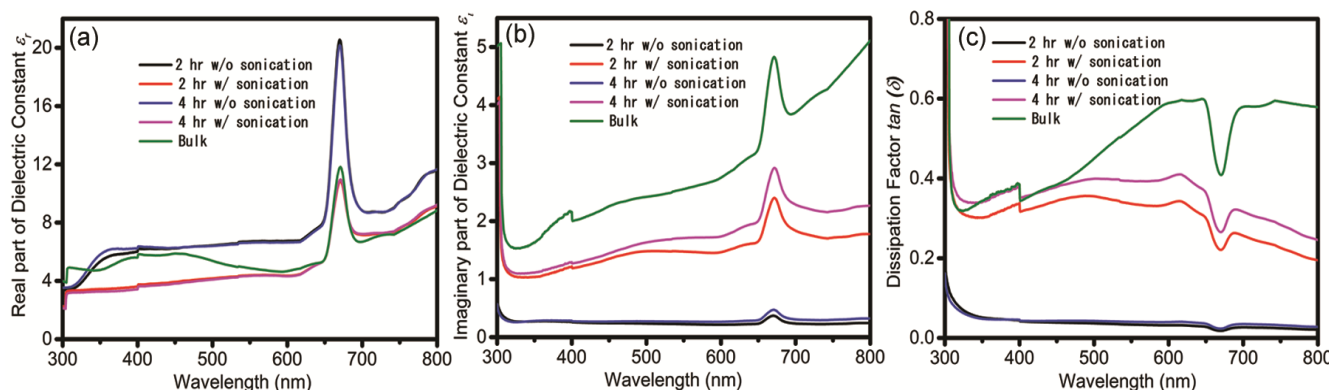


Fig. 4 — (a) Real part, (b) imaginary part of dielectric constant, & (c) dissipation factor of bulk and exfoliated MoS<sub>2</sub>.

### 3.7 Dielectric constant and dissipation factor

The dielectric constant (real part,  $\epsilon_r$ , and imaginary part,  $\epsilon_i$ ) is computed using Eq. (5) and the dissipation loss (Fig. 4c) is obtained from Eq. (6).<sup>2</sup>

$$\epsilon_r = \eta^2 - K^2 \text{ and } \epsilon_i = 2\eta K \quad \dots (5)$$

$$\tan(\delta) = \frac{\epsilon_i}{\epsilon_r} \quad \dots (6)$$

Figure 4(a) shows that the real part of the dielectric constant replicates the refractive index due to the low values of extinction coefficient. It reflects its pivotal role in selection of materials for optical properties as it varies with slight changes in refractive indices.

The real dielectric constant  $\epsilon_r$  deals with the dispersive behaviour of the materials. Fig. 4(b) shows that the imaginary part of dielectric constant  $\epsilon_i$  depends more on extinction coefficient  $K$ . The variation in  $\epsilon_r$  and  $\epsilon_i$  with wavelength signifies the possible photon-charge carriers' interaction. It is evident that the maxima of  $\epsilon_r$  (value 10.5) and  $\epsilon_i$  (value 2.9) and minima of dielectric loss (value 0.3) all occur at UV exciton peak A at 670 nm characteristic of MoS<sub>2</sub> for smallest direct transition from VB to CB. Based on the above acquired behavior of the optical parameters, it can be inferred that (i) some improvement in the optical properties of MoS<sub>2</sub> nanosheets is achieved on increasing the grinding hours from 2 hours to 4 hours, and (ii) sonication effects are more effective than grinding hours in producing few-layer MoS<sub>2</sub> as it results in greater change in the optical characteristics of MoS<sub>2</sub> nanosheets. Thus, longer grinding

hours along with sonication is promising in efficient exfoliation of MoS<sub>2</sub> in few-layer range.

### 4 Conclusion

2D MoS<sub>2</sub> nanosheets are synthesized using grinding-assisted liquid exfoliation method for varying grinding hours and sonication. No structural deformations are observed on undergoing through high energy ultrasonication process. Further, the optical properties of the nanosheets are not greatly impacted by increasing the grinding hours from 2 to 4 hours, however, sonication affects greatly towards improved optical characteristics. Subsequently, this work can be insightful for tailoring the optical properties of 2D MoS<sub>2</sub>.

### Acknowledgement

The authors acknowledge the central instrumentation laboratory, J.C. Bose University of Science and Technology, YMCA, Faridabad, India, for providing the characterization facilities.

### References

- 1 Shweta, Singh V, Kumar K, Yarramaneni S, & Kumar A, *ECS J Solid State Sci Technol*, 12 (2023) 031009.
- 2 Tiwari P, Jaiswal J, & Chandra R, *Vacuum*, 198 (2022) 110903.
- 3 Yim C, O'Brien M, McEvoy N, Winters S, Mirza I, Lunney J G, & Duesberg G S, *Appl Phys Lett*, 104 (2014) 103114.
- 4 Sun J, Li X, Guo W, Zhao M, Fan X, Dong Y, Xu C, Deng J & Fu Y, *Crystals*, 7 (2017) 198.
- 5 Gupta D, Chauhan V, & Kumar R, *Inorg Chem Commun*, 121 (2020) 108200.
- 6 Tyagi S, Kumar A, Singh M, Sanger A, & Singh B P, *Opt Mater (Amst)*, 113 (2021) 110848.

- 7 Islam K M, Synowicki R, Ismael T, Oguntoye I, Grinalds N, & Escarra M D, *Adv Photonics Res*, 2 (2021) 2000180.
- 8 Hu J-Q, Shi X-H, Wu S-Q, Ho K-M, & Zhu Z-Z, *Nanoscale Research Letters*, 14 (2019) 1.
- 9 Das S, Tama A M, Dutta S, Ali M S & Basith M A, *Mater Res Express*, 6 (2019) 125079.
- 10 Wang C, Frogley M D, Cinque G, Liu L Q, & Barber A H, *Nanoscale*, 6 (2014) 14404.
- 11 Nguyen, T P, Van Le Q, Choi K S, Oh J H, Kim Y G, Lee S M, Chang S T, Cho Y H, Choi S, Kim T Y, & Kim S Y, *Sci Adv Mater*, 7 (2015) 700.
- 12 Karmakar S, Biswas S, & Kumbhakar P, *Opt Mater (Amst)*, 73 (2017) 585.
- 13 Gaabour L H, *AIP Adv*, 11 (2021) 105120.
- 14 Parida A, Alagarasan D, Ganesan R, Bisoyi S, & Naik R, *RSC Adv*, 13 (2023) 4236.